Detection of Failures within Transformers by FRA using Multiresolution Decomposition

Jimmy C. Gonzales, *Student Member, IEEE*, Enrique E. Mombello, *Senior Member, IEEE*

Abstract—The detection of failures within power transformers is considered an important issue since these components are of critical importance for power system reliability; moreover, their replacement cost is extremely high. In monitoring the transformer condition along its useful life, Frequency Response Analysis (FRA) has gained great interest due to its sensitivity to failures in the windings and the iron core. These failures can be detected evaluating transfer function changes by means of statistical and mathematical indexes and classified according the frequency band in which these changes take place. However, this procedure involves evaluation inaccuracies due to disturbances or minor changes during FRA measurements. The new methodology is based on the decomposition of the original responses in several levels of decomposition (filtering) using the Discrete Wavelet Transform, and the subsequent comparison using smooth versions of the responses. Fault detection is further supported with statistical indexes calculated using the frequency band where abnormal differences appear. This procedure gives more robustness to the method and reduces the possible influence of disturbances during measurement in the diagnosis result. The methodology has been tested using different failure cases and two of them are used for validation purposes in this paper.

***Index Terms*—Power Transformers, Frequency Response Analysis, Discrete Wavelet Transform, Transformer Diagnosis.**

I. INTRODUCTION

The transformer is an essential component of power systems and consequently a frequent monitoring of its internal condition is necessary to prevent severe failures. Faults in transformers usually develop from slight winding deformations caused by electrodynamic forces, which reduce their strength to withstand future mechanical stresses. These kinds of deformation such as winding buckling or conductor tilting are very difficult to detect with conventional diagnostic techniques. Fig. 1 shows a severe case of winding buckling.

In recent years, the FRA technique gained popularity because of its sensibility to failures, such as winding displacements, deformations and electrical failures [1]. Failure interpretation is a very important issue to be solved in FRA diagnosis, and several methodologies for this task have been proposed [2], [3].

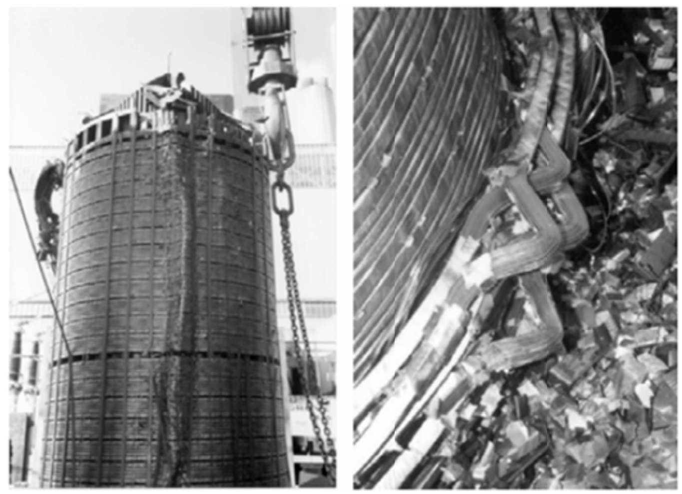

Fig. 1 Buckling of the inner LV winding.

Some of these methodologies are based on transformer modeling, which propose a circuit model to reproduce the FRA measurement. These models are sensitive to failures like winding buckling, displacements and short-circuited turns, and they have been used mainly for sensitivity analysis. This strategy has two disadvantages. On the one hand, the required frequency response accuracy to build a circuit model for failure detection analysis is rather high, so that the frequency response fitting must be very precise. On the other hand, a failure detection methodology based on the correlation between different faults and the respective variations of the equivalent circuit parameters including the definition of detection limits has not been established yet [4], [5].

Other FRA diagnosis methodologies are based on the assessment of transfer functions by means of statistical and mathematical indicators which are evaluated in several frequency bands, which are normally defined by experience [6], [7]. The definition of these frequency bands is a limitation of this methodology. Fixed frequency bands cannot be suitably defined due to the complexity of FRA measurements and the differences between FRA measurements on transformers of different type. Even in the case of twin transformers there are small construction differences affecting FRA measurements. Consequently, the frequency band limits for the development of a methodology for FRA response interpretation should be defined on the basis of the frequency response of the particular case to be analyzed.

There are some proposals for the assessment of FRA measurements which define the frequency bands by decades and evaluate the mathematical indicators using these bands

J. C. Gonzales is with the Deutscher Akademischer Austauschdiest (DAAD), E. E. Mombello and is with the CONICET and the Instituto de Energía Eléctrica – Universidad Nacional de San Juan, Av. Lib.General San Martín 1109 Oeste, J5400ARL, San Juan – Argentina (e-mails: jgonzales@iee.unsj.edu.ar, mombello@iee.unsj.edu.ar).

[5]. However, the analysis using this methodology could be misleading, since the calculated values of the mathematical indicators are affected by the ratio of the number of measurements made within the disturbed frequency region to the number of measurements in the whole decade or in the fixed frequency band used for the analysis.

This paper presents a novel methodology for FRA transformer failure detection in order to overcome the mentioned limitations using a smoothing process by applying Discrete Wavelet Transformer Analysis. This work is organized in the following manner. The characteristics of sweep frequency response analysis (SFRA) and the possible abnormalities in the frequency responses are analyzed in Section II. Section III gives the diagnosis strategy of the proposed methodology. The selection of the highest decomposition level for this application is performed in Section IV using the Min-Max index. The calculation of the limits for failure detection is shown in Section V, and the mathematical indicators for recognition of FRA trace differences are also analyzed. The methodology is validated in Section VI. Concluding remarks are given in Section VII. An Appendix is presented in Section VIII. A basic introduction to the continuous and discrete wavelet transforms and their application to FRA responses is given in Subsection VIII A. Subsection VIII B analyzes the comparison process of FRA responses using the discrete wavelet transform, and the highest theoretical differences between smoothed responses in each decomposition level are defined. Subsection VIII C presents the characteristics of the several mother wavelets from which the most suitable mother wavelet for frequency response decomposition is selected.

II. SWEEP FREQUENCY RESPONSE ANALYSIS

FRA is a transformer diagnosis technique based on the measurement of the frequency response at two different moments in the transformer service life, which are then compared to assess the transformer condition. In the particular case of SFRA, measurements are made directly in the frequency domain.

Two terminal pairs of the transformer are chosen as input and output, normally according proposed measurement layouts or standardized tests [1], [2]. The ratio of both output-input signals is considered as the response of the system to a frequency varying signal, the so-called transfer function of the transformer for a given test layout (see Fig. 2).

The normally used frequency range for this application is 20Hz to 2MHz. In this frequency range it is possible to detect electrical and mechanical failures and disturbances during the test. Measurement setup changes can also be detected above 1MHz.

Since power transformers can be modeled by means of an electrical network of inductances, resistances and capacitances, changes in these parameters produce changes in the form of the transfer function trace in some frequency bands. This characteristic is the main principle of FRA method, which is applied to the comparison between two transfer functions of the same transformer.

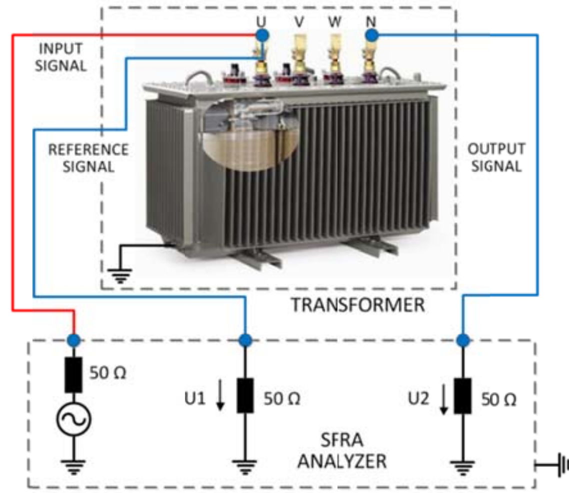

Fig. 2 FRA measurement layout.

The transfer functions to be compared are normally obtained at different times of transformer service life. In comparing FRA measurements, it is possible to find slight differences, which are not to be necessarily considered as an abnormal condition of the transformer. On the other hand, if noticeable changes in FRA traces are found, it normally reveals a possible displacement or deformation.

There are two transfer function definitions commonly used in this context: voltage ratio of response to source voltage signals, and output admittance as the ratio of output current to source voltage signals.

FRA test types have been classified by CIGRE as follows: end-to-end open circuit test, end-to-end short circuit test, capacitive inter-winding test and inductive inter-winding test [1]. The end-to-end open circuit test is the most commonly used test in transformer diagnosis because of its simplicity and the possibility to examine each winding separately [1], [2].

Transfer functions of high voltage windings normally look like the ones depicted in Fig. 3. This figure shows the reference and present transfer functions and the differences between them. If marked differences in the responses are found, it normally means that the power transformer active part has some problems or perhaps that the measurement conditions were not identical in both measurements.

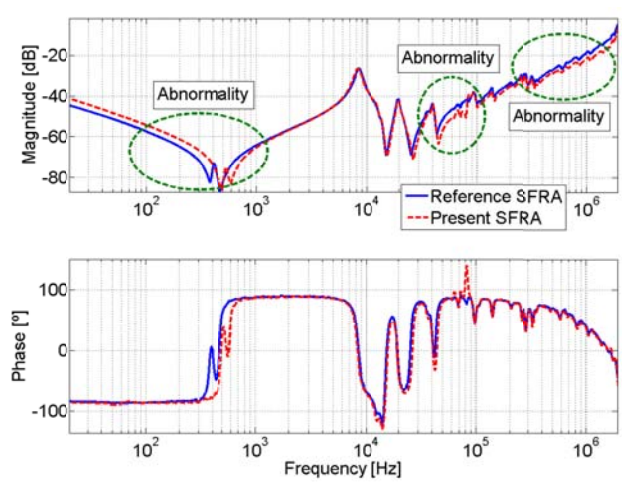

Fig. 3 Power transformer frequency responses comparison.

Measurement disturbances can also appear in the frequency response. Sometimes these disturbances produce noticeable differences by the comparison of transfer functions which can be mistaken for internal transformer failures. A procedure to avoid the effect of these disturbances is an important issue to be considered in transformer condition assessment by FRA.

The disturbances present in measured frequency responses may be classified in two types: the first one has a relatively low magnitude but contaminates the whole signal, and the second one has a relatively high intensity but exists only locally. The first one is normally due to changes in the measurement layout and connections; the second one is normally related to electromagnetic disturbances that locally affect the transfer function (external influences). A good review on this topic and other aspects of the practical application of SFRA can be found in [8], [9].

The first type of noise is well characterized by a Gaussian noise model. In this work the second type of noise is referred to as *outliers* in a sense that it is neither part of the true signal nor a minor measurement error that can be reasonably modeled by Gaussian noise [9]. Most of the noise-removal algorithms, however, do not remove well a Gaussian noise *and* outliers simultaneously. For example, the Fourier-based filtering does not work well on the outlier removal; the energy of an outlier spreads over a wide frequency range so that usual low-pass filtering cannot remove outliers efficiently.

The Wavelet Transform has recently gained in popularity in applications such as disturbance elimination and data smoothing. The related theory is given in the Appendix (Section VIII).

III. Proposed diagnosis strategy

The rationale behind the decomposition of FRA responses using DWT is to create smoothed transfer function versions with different levels of information, in order to improve the detection process of signal differences for different frequency regions.

A. Basic Assumptions and Facts

The main assumptions for the development of the new methodology are listed below:

1. Application of FRA for transformer diagnosis: It is assumed that a mechanical change or an electrical fault in the active part of the transformer produces variations in the frequency response. This is the basic assumption for FRA to be considered as a diagnostic tool. It is further assumed that the larger is the change in the transformer; the larger is the change in the transfer function.
2. In the diagnosis process, FRA measurements to be compared are generally performed under different conditions and at different times. There exist the possibility that the reproducibility is not good and there can be differences between compared measurements which are not due to variations in the transformer but to the variation of the measurement conditions.
3. The disturbances in FRA traces due to changes in the measurement conditions mainly occur in the high frequency region, which can usually be observed as superimposed fast variations or as outliers (these last ones anywhere in the trace). It is desirable that such differences are not erroneously identified as faults during the diagnosis.
4. To avoid the influence of changes in the measurement conditions it is convenient to compare smoothed versions of the transfer functions, so that any disturbances are either not present or minimized to some extent. Since the filtering process also minimizes the effects of an actual fault or change, the comparison should be made with an appropriate strategy.
5. The new comparison strategy proposes the use of several smoothed versions of the measured transfer functions with increasing degree of smoothing, to be compared by pairs. It was established that the maximum level of smoothing should be 7 for this application (see section IV).
6. It is assumed that the detection has a higher degree of certainty if it occurs at a higher smoothing level. That is why the algorithm starts comparing at level 7.

The processing of changes in FRA trace for different frequency regions and for different decomposition levels is the key factor to add robustness to the fault detection process.

B. Diagnosis Methodology Procedure

The proposed methodology has the following steps:

1. *FRA responses smoothing*: The decomposition process of FRA responses (trace smoothing) is performed by applying the Discrete Wavelet Transform. Both present and reference responses undergo successive smoothing steps, obtaining seven smoothed versions of the original transfer functions, denoted as (L1, L2,..., L7) for increasing decomposition level. The frequency range used is 20 Hz - 2 MHz. The functions obtained from the present and reference responses are compared for each decomposition level following a particular procedure.
2. *Comparison procedure of FRA responses*: The comparison of smoothed versions of present and reference responses is done starting with L7 and then continuing with the successive levels in decreasing order. For a given decomposition level, the analysis is performed from low to high frequencies, using the logarithmic scale for the abscissa (frequency), which produces an expansion of the response trace at low frequencies and a compression at high frequencies. In the case that the comparison leads to abnormal differences in a given decomposition level, the frequency bands containing these abnormal values are stored and not rescanned when comparing traces at lower decomposition levels. This is because the corresponding detection limits of all smoothing levels are defined in such a way that if the detection occurs in one level, this will also occur at lower levels. Thus the detection takes place through the comparison of the "most representative components" of the responses, i.e., the components that remain after the filtering process, leaving aside response trace components having fast variations, which are to be compared at lower decomposition levels. This ensures that the detection of an abnormal difference is due to an actual failure, since a deviation arises in the basic form of the compared responses, and not from differences due to noise.

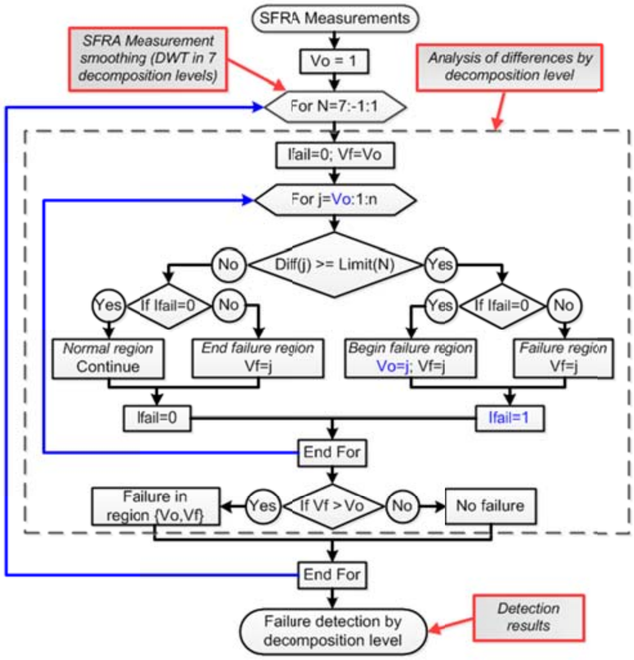

Fig. 4. Graphical representation of the proposed procedure.

A graphical representation of the proposed procedure is given in Fig. 4, where N is the current decomposition level, Diff is the difference vector with n components, V_0 and V_f are the indexes for the lower and upper limits of the failure zone k (k=1, 2,…), if any, and Ifail is an auxiliary variable that checks if a failure region is detected in the region between V_0 and V_f. For simplicity's sake, the chart of Fig. 4 considers only one failure zone by level. The left part of the chart (to the left of the first comparison block) is the flow path as long as no failure is detected. As soon as a failure region is found, the flow changes to the right side and the failure start index (V_0) is set. The flow remains at this side as long the failure is present. When the first measurement below the limit is found, the flow returns to the left side and the failure end index (V_f) is set. The application of this procedure to a real case is shown in Fig. 5. In this example two frequency bands with failure were detected in different decomposition levels (N=7, N=5).

3. *Detection of abnormalities*: The L7 smoothed versions of the present and reference transfer functions are initially compared to detect abnormalities. In this level, any abnormality can only represent a failure, since the effects of external disturbances and measurement problems have been extremely filtered. The comparison begins at 20 Hz and continues toward higher frequencies, checking if the limit for failure differences established for this decomposition level (1.42 dB for L7 for measurements in the same phases) is exceeded or not. Difference limits for the remaining decomposition levels are also necessary, since the smoothing levels are different (see Section V). In case of detecting abnormal differences in a given frequency band, it is stored as an abnormal band for that level of decomposition and the upper limit of this frequency band is set as the starting frequency for the comparison in the next level of decomposition.

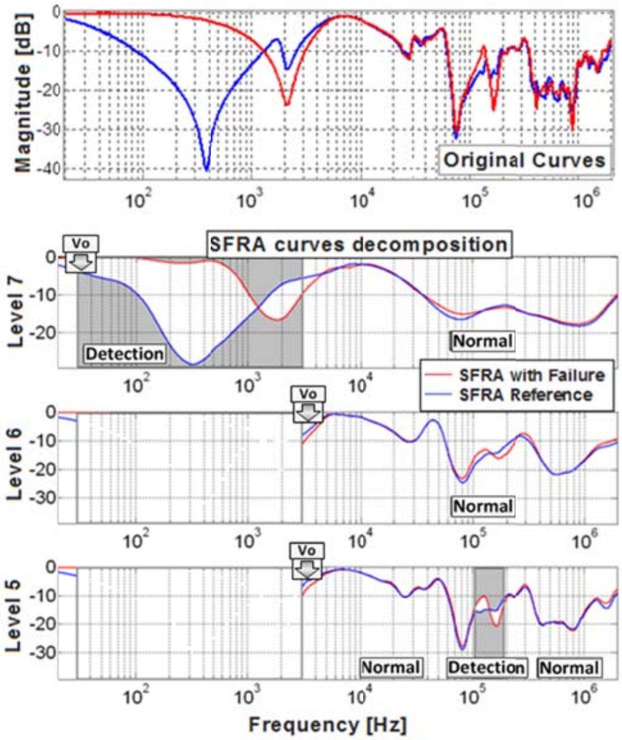

Fig. 5. Application example of the proposed procedure.

If no abnormalities are detected, the starting frequency value remains the same for the next search. The comparison continues this way up to the first decomposition level (L1), where the comparison process ends.

4. *Complementary diagnosis using mathematical indicators*: The frequency bands containing abnormal differences (differences exceeding the limits) detected in each decomposition level are to be analyzed using mathematical indicators to determine if they are correlated to a failure or not. The indicators used in this methodology are the correlation coefficient (CC) and the min-max index (MM). The application of this step adds robustness to the method. Note that the indexes are applied only to the frequency region containing abnormalities and not to the whole frequency range, so that the sensitivity increases.
5. *Definition of dynamic ranges for a given frequency response*: To identify the type of failure it is important to divide the frequency range in frequency bands, since a given type of fault is usually detected at a certain frequency band [2], [5]. While fixed frequency bands have been used in the past, this is not optimal because its applicability varies with the shape of the given transfer function. To avoid this, a subdivision in frequency bands whose limits are based on the characteristics of the FRA response of a given case study should be used, as explained in [10].
6. *Fault identification*: Based on the results obtained in previous stages, the type of fault can be investigated and identified according to the frequency band where the abnormality occurs.

It should be noted that steps 5 and 6 have been added for the sake of completeness, since these steps are out of the scope of this paper. These steps are an important part of the procedure and they are to be dealt with in a companion paper.

IV. Determination of the Number of Decomposition Levels

The criterion to choose the adequate number of decomposition levels is based on the analysis of the correlation and differences between original and smoothed FRA traces at low frequency ranges. The goal of this analysis is to find the maximum decomposition level for which there is still no noticeable difference between the smoothed transfer function and the original one at the low frequency region (see Fig. 7 and compare the reproducibility of levels 7 and 8 at low frequencies).

For analysis purposes, it is convenient to represent the transfer function using a logarithmic scale for the frequency axis, so that the low frequency region of the transfer function looks expanded and the high frequency region looks compressed. Consequently, the low frequency region of the curve can be associated with a smooth behavior of the trace, and the high frequency region with a rough one.

The wavelet filtering process of a FRA trace gives both low order decomposition levels, which retain smooth and fast changes in the shape of the curve, and high order levels, which only retain the background shape of the curve (smooth). The higher the decomposition level, the smoother is the filtered trace. This situation suggests that the low frequency region of the transfer function is to be better analyzed with the higher decomposition levels, the medium frequencies with the intermediate decomposition levels and the high frequencies with the lower decomposition levels. The analysis is therefore performed from low to high frequencies (see Fig. 6).

The decomposition procedure is applied to the frequency response magnitude expressed in decibels and to the phase in degrees, and the spot frequencies of the frequency scale are stored as a frequency position vector (logarithmic). The decomposition is done using the *Daubechies* mother wavelet of 6th order (similar results are obtained using *Symlet* wavelet, see Appendix). The calculation of the differences and correlations is done using the min-max index given in (1) [11].

$$MM(y_1, y_2) = \frac{\sum_{i=1}^{N} Min(|y_{1i}|,|y_{2i}|)}{\sum_{i=1}^{N} Max(|y_{1i}|,|y_{2i}|)} \quad (1)$$

where y_{1i} and y_{2i} are the original and the smoothed transfer functions, respectively. The results of MM application are shown in Fig. 7. The smoothing applied to the transfer function is adequate until the 7th decomposition level, since for low frequencies (between 20Hz and 120Hz) is MM=0.9432, that represents a suitable approximation.

Note that the 7th decomposition level is used to analyze the low frequency range of the FRA trace. For the 8th level the value is MM = 0.5911, which means that there is no correlation and the approximation is bad. It can be concluded from the analysis of this case and many other ones, that seven decomposition levels are adequate for the smoothing process in the frequency range between 20 Hz and 2 MHz.

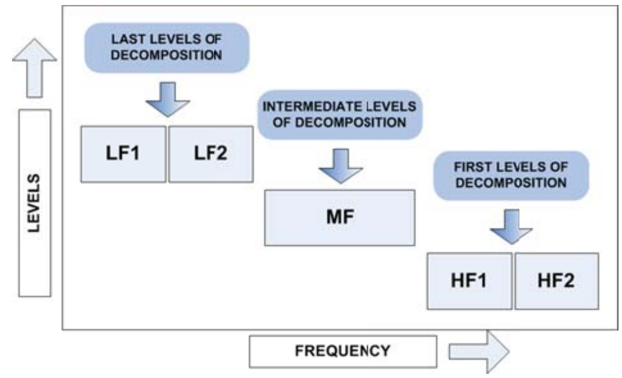

Fig. 6. Decomposition level analysis against frequency range.

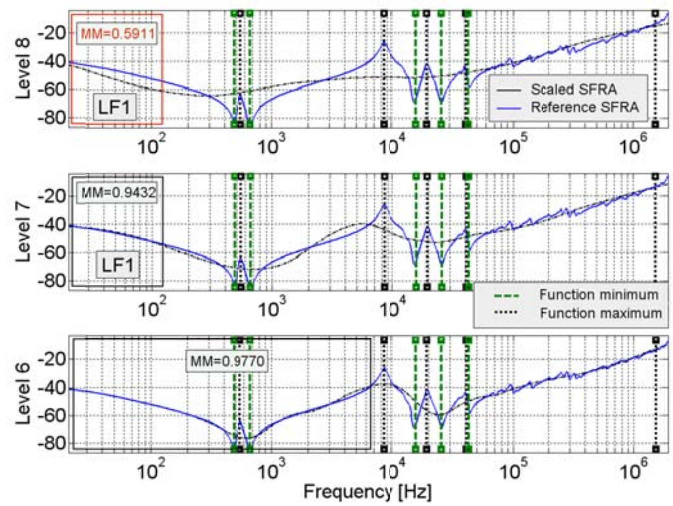

Fig. 7. Suitable decomposition levels determination for FRA analysis.

V. Definition of Limits for Failure Analysis: Frequency Response Differences and Mathematical Indicators

In order to perform the comparisons of the smoothed versions of the present and reference FRA traces in each decomposition level, tolerance limits for each level are necessary.

The limit of the differences between reference and present transfer functions at level i is called $[\Delta i]_{limit}$. It can be shown that these limits can be estimated for each decomposition level from the maximum difference in the higher decomposition level Δ_M (i.e., the 7th level). For the last decomposition level, the analyzed functions are strongly smoothed, so that the differences obtained from comparison should be minimal. During the comparison of two smoothed transfer functions of a sound transformer in a given decomposition level, the differences are normally below a certain limit and they are compatible with a normal condition and a good measurement procedure. However, in some cases these differences can be strongly affected by external perturbations and their distribution in each decomposition level is irregular. Therefore, it is necessary to find the decomposition level for which the values of these perturbation limits are minimal, and this is obviously the higher decomposition level (7th level).

Consequently, the 7th decomposition level is used to define the limit of the differences for good measurements and also the limit of measurements with failure. In order to have coherent limits in each decomposition level, the limits for the other levels are derived from the limit for the 7^{th} level by means of the dyadic scale by using (21).

The differences found in the compared frequency responses can be classified in three groups. Differences are *normal* when the quality of the measurement is good and the differences are below a certain limit, which is called limit N. Differences are *marginal* when some perturbation is present in the measurement or also other differences not related to a failure, which do not exceed the limit F. The differences that exceed the limit F are considered as possible *failure*. These concepts are shown schematically in Fig. 8. The same criterion is used for the classification of compared responses according the mathematical indicators.

The limits N and F for the last (7^{th}) decomposition level (i.e., Δ_M) are to be calculated first. These limits (Δ_M) have been estimated on the basis of 21 real FRA (end-to-end open) measurements on power transformers in normal and abnormal condition (see Tables 1 and 2).

Table 1. Limits of differences in the same phases (7^{th} level)

Good Measurement	Marginal Measurement	Failure
±0.60-0	±1.42±0.60	>±1.42

Table 2. Limits of differences in different phases (7^{th} level)

Good Measurement	Marginal Measurement	Failure
±0.94-0	±2.00±0.94	>±2.00

The calculation has been done by determining the highest differences between transfer functions smoothed to the 7^{th} decomposition level. The limits for lower decomposition levels (6^{th},…, 1^{st}) are calculated using (21). The limits are shown in Fig. 9 for comparison between measurements on the same phases and also for measurements on different phases.

It is important to mention that in the case of comparing measurements on different phases, there are structural differences between lateral and central phases and consequently there exist transfer function differences most located in the low frequency range below 1 kHz (+3dB) that needs to be considered during the comparison.

The analysis of the frequency response differences is done by considering the two most common mathematical indicators used in the bibliography, the min-max index, already given in (1), and the correlation coefficient, defined in (2) [3].

$$CC(y_1, y_2) = \frac{\sum_{i=1}^{N} y_{1i} y_{2i}}{\sqrt{\sum_{i=1}^{N} y_{1i}^2 \sum_{i=1}^{N} y_{2i}^2}} \qquad (2)$$

The correlation coefficient gives the degree of similarity, so that its value is close to 1 if the shape of y_1 is similar to that of y_2, and close to 0 if not. A disadvantage of this indicator is its insensitivity to constant differences between the transfer functions being compared, since the correlation coefficient is a normalization of the covariance between two data records.

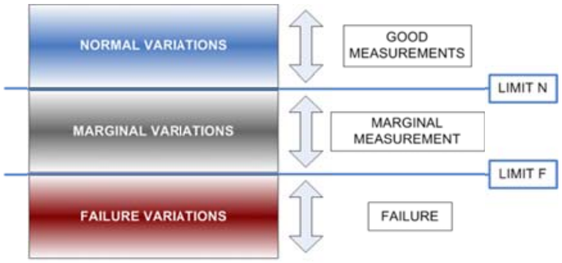

Fig. 8. Limits for the differences between compared curves.

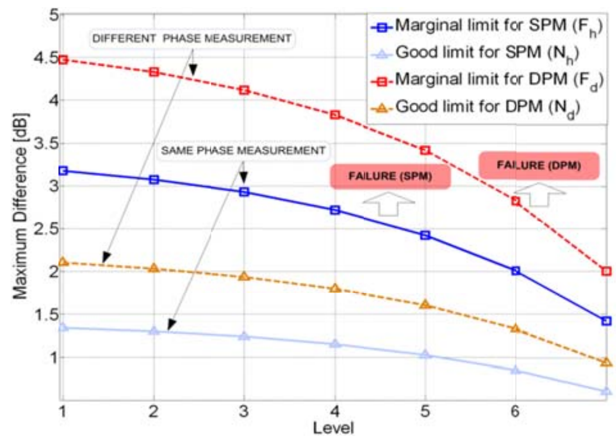

Fig. 9. Highest differences in FRA analysis for measurements on the same phases (SPM) and on different phases (DPM).

The min-max indicator makes it possible to identify the degree of similarity between two vectors (i.e., FRA traces), and it is sensitive to constant differences. The min-max and correlation coefficient indicators are used as an additional tool in order to enhance the robustness of the diagnosis.

These indicators have been also evaluated using 21 FRA measurements and the limits shown in Tables 3 and 4 have been found.

Table 3. Limits of CC and MM for measurements on the same phases

Good Measurement		Marginal Measurement		Failure	
CC	MM	CC	MM	CC	MM
1-0.99	1-0.97	0.99-0.98	0.97-0.91	<0.98	<0.91

Table 4. Limits of CC and MM for measurements on different phases

Good Measurement		Marginal Measurement		Failure	
CC	MM	CC	MM	CC	MM
1-0.98	1-0.89	0.98-0.97	0.89-0.88	<0.97	<0.88

VI. Validation

The proposed methodology has been validated using two different transformer failure cases. The first case is a mechanical failure, for which the abnormalities are present at high frequency ranges, and the second case is an electrical failure, showing a different frequency response behavior at low frequencies. The failures were identified through visual inspection in both cases, revealing a winding conductor tilting in the first case, and a short circuit to ground of internal connections in the second case.

The analysis of both cases show the advantages of the new methodology, and the results are compared with the assessment achieved by means of the Chinese standard for SFRA transformer diagnosis [12], which is the only standard currently in force (not for western countries) and used as an computer-assisted diagnosis tool in many commercially available SFRA analyzers.

Case A: The first case analyzed consists of measurements on the same phase (phase A) of the LV winding of a 100 MVA, 550/230/14 kV transformer. The analysis has been done using the measurements on phase A, as shown in Fig. 10. It can be seen from Fig. 11 that the transfer function magnitude shows a possible failure evidenced as trace shifts in the frequency range above 50 kHz.

The evaluation of the differences and interpretation according to the Chinese standard consists in the analysis by means of the Relative Factor R [12]. This factor is evaluated at fixed frequency bands, as indicated in Table 5. The values of the Relative Factor in the corresponding frequency bands defined in Table 5 are shown in Fig. 11 for the present case. The diagnosis by the Chinese standard gives a normal condition of the winding. However, this result does not agree with the visual inspection of the transformer.

The application of the proposed methodology to the same transformer is depicted in Fig. 12. The comparison in the 4th decomposition level leads to a failure detection in the frequency region between 18 kHz and 388.60 kHz (shaded region). In lower decomposition levels no failure has been found. Above 1MHz, abnormalities have not been detected, correlating the small differences to disturbances in the measurements. The failure detection by the new procedure corresponds to the visual inspection of the transformer. The white box at level 2 means that this region should not be considered in the analysis al levels lower than the 4th level.

Case B: Measurements on the same phase (phase A) of the HV winding of a 100 MVA, 550/230 kV power transformer has been considered as the second case study. The frequency responses are shown in Fig. 13. It can be seen that the transfer functions show a possible failure evidenced as trace shifts in the frequency range between 300 Hz to 10 kHz.

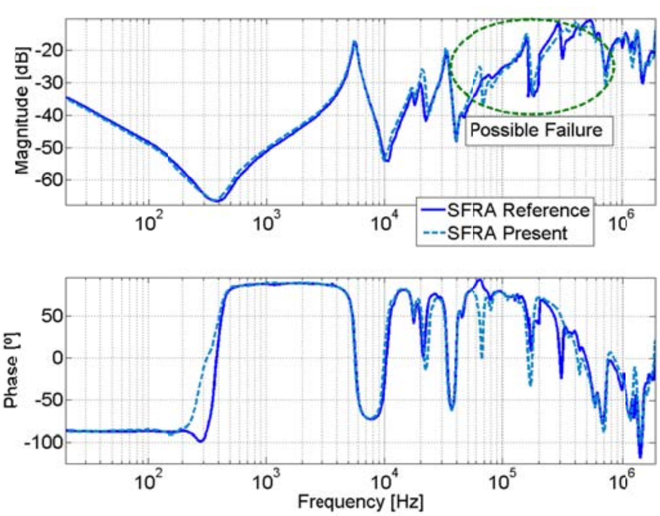

Fig. 10. FRA measurements on 230kV power transformer winding.

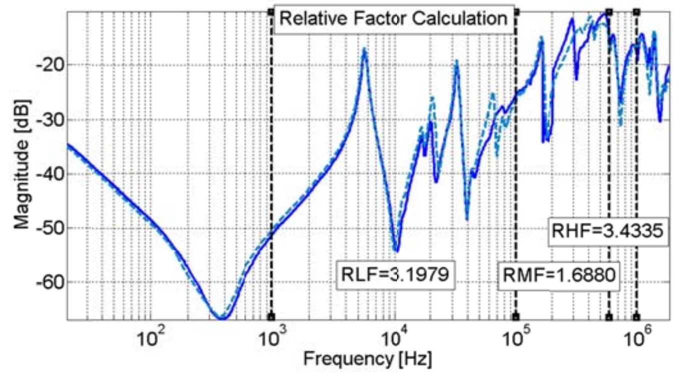

Fig. 11. Relative Factor Calculation for case A.

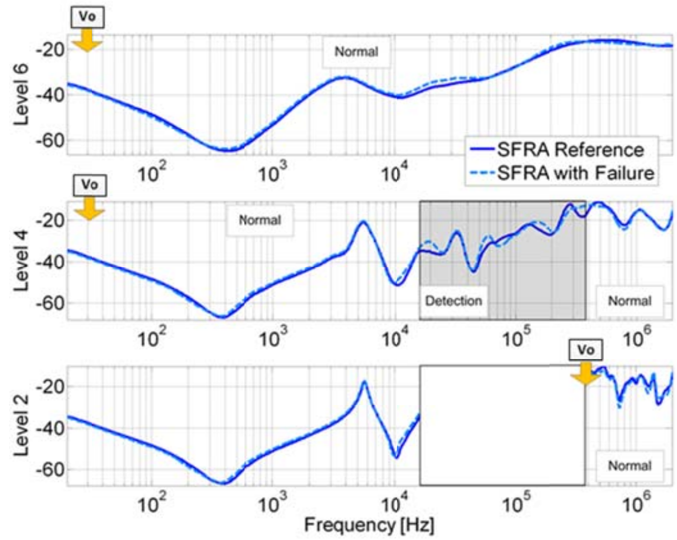

Fig. 12. FRA measurements on a 230kV power transformer winding.

Table 5. Relative Factor and degree of winding deformation

Degree of winding deformation		Relative Factor
Serious deformation		RLF<0.6
Obvious deformation		1>RLF≥0.6 or RMF<0.6
Slight deformation		2>RLF≥1 or 0.6≤RMF<1
Normal condition		RLF≥2, RMF≥1 and RMF≥0.6
Note	**RLF** for low frequencies (1kHz~100kHz) **RMF** for medium frequencies (100kHz~600kHz) **RHF** for high frequencies (600kHz~1MHz)	

Above 1 MHz, abnormalities have not been detected, correlating the small differences to disturbances in the measurements. The failure detection by the new procedure corresponds to the visual inspection of the transformer.

The evaluation of the analyzed transfer functions using the Relative Factor R is shown in Fig. 14. The relative factor calculation shows that this case corresponds to a normal condition of the winding, but the visual inspection of the power transformer shows a failure. The application of the proposed methodology is depicted in Fig. 15.

The comparison in the 6th decomposition level leads to a failure region detection in the frequency region between 200 Hz and 7.2 kHz. In the 4th decomposition level another failure region is detected in the frequency range between 7.2 kHz-10 kHz. No failure has been found in the remaining decomposition levels.

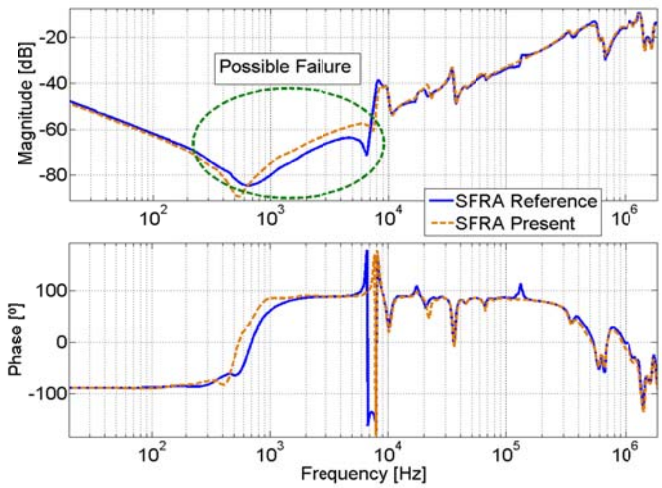

Fig. 13. FRA measurements on 550kV power transformer winding.

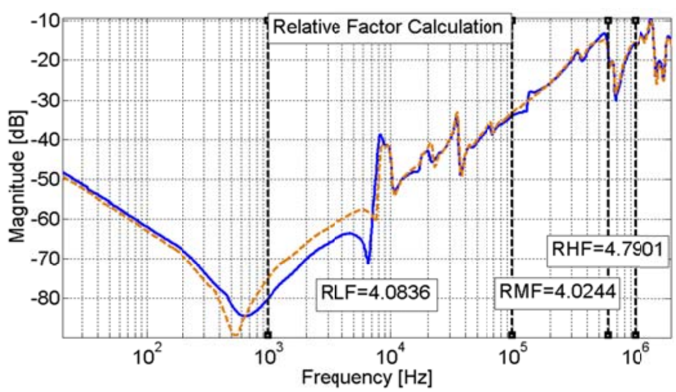

Fig.14. Relative Factor Calculation for case B.

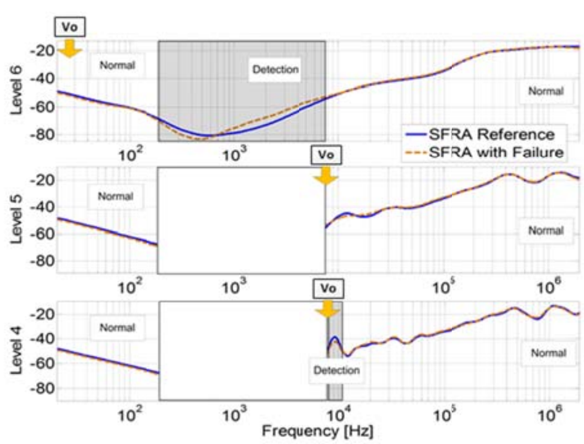

Fig. 15. FRA measurements on a 550 kV power transformer winding.

In both analyzed cases the failures have been clearly detected, which shows an improved detection performance of the new methodology.

VII. Conclusions

A new methodology for failure detection has been proposed, based on the use of DWT smoothed versions of the original frequency response containing basic shapes with increasing detail as the level decreases, which is a strategic DWT application for failure recognition

The new methodology can reliably detect transformer failures avoiding the influence of possible disturbances due to differences in the measurement setup and external influences that can interfere with the analysis.

The improved accuracy for failure detection of the new methodology is based on a strategic evaluation of differences at each decomposition level. Furthermore, the transformer condition is confirmed by means of mathematical indicators calculated at the narrow frequency bands containing the detected abnormalities and not at wider and fixed frequency bands, thus adding robustness to the diagnosis.

The corresponding failure detection limits for curve differences, correlation coefficient and min-max index for each decomposition level have been proposed.

An improved methodology for failure classification to be applied along with the proposed detection procedure is to be presented in a future work.

VIII. Appendix

A. FRA response decomposition using the wavelet transform

The Wavelet Transform is a mathematical tool developed for local analysis of nonstationary and fast transient wide-band signals, which has become increasingly popular. The Wavelet Transform is a mapping of the signal $f(x)$ to the translation and scale representation that is similar to the short-time Fourier transform, the Wigner distribution and the ambiguity function. The Wavelet Transform provides multiresolution analysis with dilated windows [13], [14].

The theory is based on the idea of processing the data function $f(x)$ in every scale and different positions with a function $\psi(x)$ called "mother wavelet".

The necessary wavelet versions for every scale can be obtained from the mother wavelet according to (3).

$$\psi_{b,a} = \frac{1}{\sqrt{a}}\psi(\frac{x-b}{a}) \tag{3}$$

where the parameters a and b are the scale and position factors respectively.

The Continuous Wavelet Transform (CWT) of the data function $f(x)$ is defined through its correlation of with the wavelet $\psi_{b,a}(x)$ [14] as

$$W_f(b,a) = \left\langle f, \psi_{b,a} \right\rangle = \int_{x1}^{x2} f(x) \cdot \psi^*_{b,a}(x)dx \tag{4}$$

The Continuous Wavelet Transform applied to the complex transfer function $\boldsymbol{H(\omega)}$ is defined in (5) as explained in [9] and [15].

$$W_{SFRA}(b,a) = \frac{1}{\sqrt{a}}\int_{-\infty}^{+\infty} \overline{H}(\omega) \cdot \phi^*_{b,a}(\omega)d\omega \tag{5}$$

In order to simplify the notation, $\psi(x)$ is expressed as the conjugate of $\psi(x)$ as follows

$$\psi(\frac{\omega-b}{a}) = \phi^*(\frac{\omega-b}{a}) \tag{6}$$

Complex transfer functions are normally expressed in phasor form as

$$\overline{H}(\omega) = \left|\overline{H}(\omega)\right| \angle angle(\overline{H}(\omega)) \tag{7}$$

FRA measurement instruments usually provide these two quantities (magnitude and phase) and FRA analysis is made using this representation. The expert knowledge in FRA is based on these quantities and a mathematical tool for their processing is required.

By applying logarithms to (7), the transfer function can be expressed in two terms as follows

$$\begin{aligned}\tilde{H}(\omega) &= 20\cdot\log_{10}(\overline{H}(\omega)) \\ &= 20\cdot\log_{10}(|\overline{H}(\omega)|) + j\cdot 20\cdot\log_{10}(e)\cdot angle(\overline{H}(\omega))\end{aligned} \tag{8}$$

The real component is the magnitude of the transfer function in decibels and the imaginary component is proportional to its phase.

The decomposition of the logarithmic complex transfer function is obtained by applying the Wavelet Transform to (8) as follows

$$\begin{aligned}W_{\tilde{H}(\omega)}(b,a) &= \frac{1}{\sqrt{a}}\int_{-\infty}^{+\infty}\left\{20\cdot\log_{10}(|\overline{H}(\omega)|)\right\}\cdot\psi(\frac{\omega-b}{a})\cdot d\omega \\ &+ j\cdot 20\cdot\log_{10}(e)\cdot\frac{1}{\sqrt{a}}\int_{-\infty}^{+\infty}\left\{angle(\overline{H}(\omega))\right\}\cdot\psi(\frac{\omega-b}{a})\cdot d\omega\end{aligned} \tag{9}$$

The first term of (9) represents the transfer function magnitude decomposition in decibels and the second one is the decomposition of the complex transfer function phase, defined in (10) and (11) separately

$$W_{|\overline{H}(\omega)|} = \frac{1}{\sqrt{a}}\int_{-\infty}^{+\infty}\left\{20\cdot\log_{10}(|\overline{H}(\omega)|)\right\}\cdot\psi(\frac{\omega-b}{a})\cdot d\omega \tag{10}$$

$$W_{angle(\overline{H}(\omega))} = \frac{1}{\sqrt{a}}\int_{-\infty}^{+\infty}\left\{angle(\overline{H}(\omega))\right\}\cdot\psi(\frac{\omega-b}{a})\cdot d\omega \tag{11}$$

The Continuous Wavelet Transform, as indicated in (10) and (11), maps a one-dimensional signal to a two-dimensional translation-scale joint representation. In the variable x, or ω for FRA analysis, the bandwidth product of the Continuous Wavelet Transform output is the square of that of the signal (FRA response). For most applications, however, the goal of signal processing is to represent the signal efficiently with fewer parameters. The use of the Discrete Wavelet Transform (DWT) can reduce the variable x bandwidth as a product of the Wavelet Transform output.

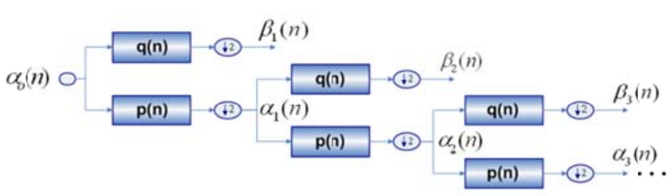

Fig. 16 Decomposition process by multiresolution analysis.

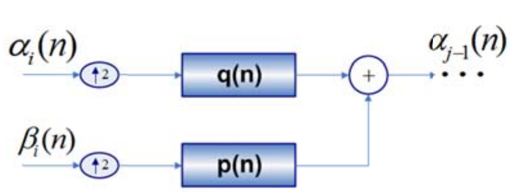

Fig. 17 Schematic representation of the reconstruction process.

The Discrete Wavelet Transform is defined by the following series

$$\begin{aligned}f(x) &= \sum_{k\in Z} 2^{-M/2}\alpha_k\,\varphi(2^{-M}x-k) \\ &+ \sum_{j=1}^{M}\sum_{k} 2^{-j/2}\beta_{jk}\,\psi(2^{-j}x-k)\end{aligned} \tag{12}$$

where $\varphi(x)$ is the smooth function and $\psi(x)$ the applied mother wavelet for the decomposition, α_k are the approximation coefficients and β_k the details.

The function $f(x)$ in (12) is represented as an approximation at resolution i=M plus the sum of M detail components at dyadic scales. The first term in the right-hand side of (12) is the smoothed approximation of $f(x)$ at very low resolution i=M. When M approaches to infinity, the projection of $f(x)$ on the scaling functions of very large scale would smooth out any signal detail and converges to a constant. The function $f(x)$ is then represented as a series of its orthonormal projections on the wavelet bases.

The definition in (12) can be expressed by multiresolution analysis through the sequences of analysis filters shown in Fig. 16, for the decomposition procedure in M levels.

The reconstruction of the original sequence α_o can be performed applying a convolution process through synthesis filters, as indicated in Fig. 17.

The data smoothing task as it has been described implies that only the approximation components are considered in (12), which means that the details are removed, thus the smoothed function version is expressed as

$$f_{smooth}(x) = \sum_{k\in Z} 2^{-M/2}\alpha_k\varphi(2^{-M}x-k) \tag{13}$$

B. Comparison of smoothed FRA responses

From the Discrete Wavelet Transform definition, i.e., the wavelet series in (12), the differences between two successive approximations can be derived as

$$\begin{aligned}\Delta f_M^{M-1} &= \sum_{k\in Z} 2^{-(M-1)/2}\alpha_k\phi(2^{-(M-1)}x-k) \\ &-\sum_{k\in Z} 2^{-M/2}\alpha_k\phi(2^{-M}x-k)\end{aligned} \tag{14}$$

They can also be expressed in terms of detail coefficients as

$$\Delta f_M^{M-1} = \sum_{k} 2^{-M/2}\beta_{Mk}\psi(2^{-M}x-k) \tag{15}$$

The decomposition differences at level M can be expressed in terms of the differences at decomposition level i as follows

$$\Delta f_M = \Delta f_i + \sum_{j=i+1}^{M}\sum_{k} 2^{-j/2}\beta_{jk}\psi(2^{-j}x-k) \tag{16}$$

Since FRA analysis in power transformer diagnosis is based on the comparison of two transfer functions, a second function $g(x)$ is considered, for which a similar expression for the differences can be written

$$\Delta g_M = \Delta g_i + \sum_{j=i+1}^{M}\sum_{k} 2^{-j/2}\beta_{jk}^{g}\psi(2^{-j}x-k) \tag{17}$$

The differences between these two differences given in (16) and (17) for the decomposition level M is given by

$$\Delta_M = \Delta_i \pm \sum_{j=i+1}^{M} \left[\sum_k 2^{-j/2} (\beta_{jk} \mp \beta_{jk}^g) \psi(2^{-j}x - k) \right] \quad (18)$$

This expression considers that the difference at a decomposition level M of two transfer functions are the differences at a decomposition level i plus the sum of the details up to level M. Conversely, it is possible to obtain the differences at level i from the differences at level M as

$$\Delta_i = \Delta_M \mp \sum_{j=i+1}^{M} \Delta_j^{j-1} \quad (19)$$

where the expression in brackets in (18) has been replaced by the definition given in (15) for the differences between two successive approximations.

The normalization for FRA transfer functions can be done using the following expression

$$\Delta_j^{j-1} = \Delta_{j+1}^{j} 2^{-1/2} \quad (20)$$

which assumes that the differences along the frequency response are distributed according the dyadic scale.

The final equation for transfer function differences is

$$\Delta_i = \Delta_M + \Delta_M (2^{1/2} - 1) \sum_{j=i+1}^{M} 2^{(M-j)/2} \quad (21)$$

This equation reveals that the differences in each decomposition level are logarithmically (dyadic) distributed from an initial value Δ_M.

In order to meet (21), FRA data measurement needs to be given in decibels (dB) and the measured frequencies as a logarithmic position vector, so that the differences are distributed logarithmically (dyadic scale).

C. Mother wavelet selection for frequency response decomposition

The following analysis focuses attention on the most common wavelets used in the bibliography, which at first glance could give good results in FRA analysis. The selected mother wavelets are in principle those which have scale functions φ*(x)* as defined for application in frequency response decomposition.

Different kinds of transfer functions have been used in order to select the best mother wavelet. It should be noted that there is almost no difference in the result of this selection if typical FRA transfer functions are used. In order to show the effects of the smoothing process of the DWT, the FRA transfer function in Fig. 3 has been used.

The performance of the most commonly used mother wavelets has been analyzed in order to choose the better option for this special application (see the list in Table 6) [16]. The version of each wavelet class which provides the better smoothing have been used for comparison. Fig. 18 shows their forms and corresponding characteristics.

The order of each mother wavelet depends on the decomposition levels required for transfer function analysis.

The analysis of the selected mother wavelets gave the results shown in Fig. 19, where the decomposition and transfer function reconstruction procedure shows no marked differences between them.

Small differences can be observed in the upper decomposition levels (above 4th level). A correlation analysis has been done between the reconstructed transfer functions and the original ones, where Daubechies and Symlet wavelets showed better performances. It is also important to note that there exists certain similarity between the frequency response shape and the mother wavelet shape in the case of *Daubechies* and *Symlet* wavelets above 6th order, which produce similar results and achieve a better reproduction of the frequency response.

Consequently, it can be concluded that *Daubechies* and *Symlet* mother wavelets have a good performance for transfer function decomposition in the case of comparing FRA measurements.

Another important issue is that the accuracy of wavelets depends on the wavelet function order. According to the analysis, the minimum suitable wavelet order for the selected mother wavelet is the 6th order.

Table 6. Mother Wavelets

Wavelet	Acronym	Order
Daubechies	db	1-10-**
Symlets	Sym	2-8-**
Haar	haar	
Coiflets	Coif	1-5

(** higher order wavelets)

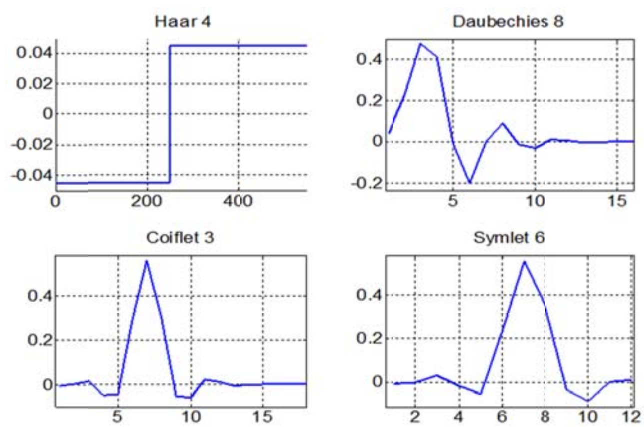

Fig. 18 Mother wavelets for FRA applications.

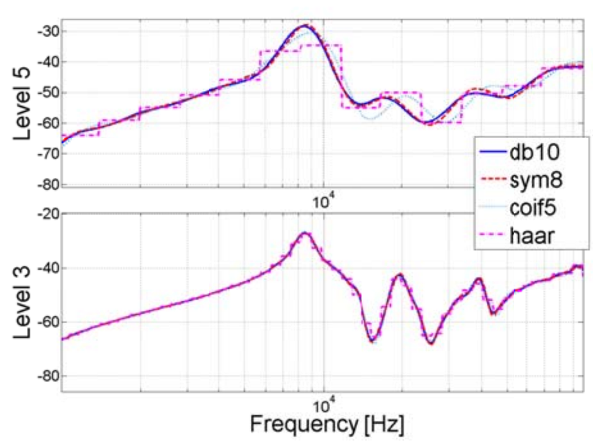

Fig. 19. Decomposition analysis applying different mother wavelets.

IX. References

[1] Working Group A2.26, "Mechanical-Condition Assessment of Transformer Winding Using Frequency Response Analysis (FRA)", CIGRE publication 2008.

[2] S. D. Mitchell, and J. Welsh, "Modeling Power Transformer to Support the Interpretation of Frequency-Response Analysis", IEEE Transactions on Power Delivery, Vol.26, No.4, pp 2705-2717, October 2011.

[3] S. A. Ryder, "Methods for comparing frequency response analysis measurements", Conference record of the 2002 IEEE International symposium on electrical insulation, Boston, MA USA, April 2002.

[4] E. Bjerkan, and H. K. Høidalen, "High frequency FEM-based power transformer modeling: Investigation of internal stresses due to network-initiated overvoltages", Electric Power Systems Research, Vol. 77, 1483–1489, 2007.

[5] J. Velasquez, and D. Kolb, "Identification of transformer-specific Frequency Sub-Bands as basis for Reliable and Automatic Assessment of FRA Result", Conference Proceedings of CMD, 2010.

[6] G. M. Kennedy, A. J. McGrail, and J. A. Lapworth, "Transformer sweep frequency response analysis (SFRA)", energize, October 2007, pp 28-33.

[7] H. Firrozi, and M. Shishehchian, "Frequency Response Analysis-Condition Assessment of Power Transformers Using mathematical and Statistical Criteria", Proceeding of the 9th International Conference on Properties and Applications of Dielectric Material, July 19-23, 2009, Harbin, China.

[8] A. Kraetge, M. Kruger, and J.L. Velasquez, "Aspects of the Practical Application of Seep Frequency Response Analysis (SFRA) on Power Transformer", 6th Southern Africa Regional Conference (CIGRE 2009), Southern Africa 2009.

[9] P. Moulin, "Wavelet Thresholding Tecniques for Power Spectrum Estimation", IEEE Transactions on Signal Processing, Vol. 42, No11, November 1994.

[10] J. C. Gonzales, and E. E. Mombello, "Automatic Detection of Frequency Ranges of Power Transformer Functions for Evaluation by Mathematical Indicators". IEEE PES T&D LA 2012. Montevideo, Uruguay. September 2012.

[11] J. Secue, "Methodologia para el diagnostico de fallas en los devanados del transformador de potencia en base al análisis de respuesta en frecuencia", doctoral thesis, Universidad Nacional de San Juan, Argentina, 2009.

[12] "Frequency Response Analysis on Winding Deformation of Power Transformers", The Electric Power Industry Standard of People's Republic of China, Std. DL/T911-2004, ICS27.100, F24, Document No. 15182-2005, June 1st, 2005.

[13] I. Daubechies, "Ten Lectures on Wavelets", Society for Industrial and Applied Mathematics, Philadelphia, Pennsylvania, 1992.

[14] Y. Sheng, "Wavelet Transform", in The Transforms and Applications Handbook, 2nd ed., Chap. 10, A. D. Poularikas, Ed., CRC Press and IEEE Press, 1999.

[15] H. P. Yin, "Natural frequencies and damping estimation using wavelet transform of frequency response function", Journal of Sound and Vibration, Vol. 271, pp 999–1014, 2004.

[16] J. Martinez, and R. M. Fernandez, "Analisis de la teoria de ondículas orientada a las aplicaciones en ingenieria eléctrica: Fundamentos", E. T. S. Industriales, Electrical Ingineering Department, Madrid 1995.

X. Biographies

Jimmy Cesar Gonzales Arispe (S) was born in Cochabamba, Bolivia on April 26, 1984. He received the electrical engineer degree from Universidad Mayor de San Simón (UMSS), Bolivia, in 2006. He is currently pursuing the Ph.D degree at Universidad Nacional de San Juan (UNSJ), as part of scholarship financed by Deutscher Akademischer Austauschdienst (DAAD). Mr. Jimmy is a member of the IEEE Power Engineering Society. His research interests are power transformers and power quality.

Enrique Esteban Mombello (IEEE M'95-SM'00) was born in Buenos Aires, Argentina, in 1957. He received the B.S. degree in electrical engineering and the Ph.D. degree in electrical engineering in 1982 and 1998, respectively. He has more than 30 years of experience in research projects which include topics like electrical transients and resonance processes within transformers as Researcher of the National Council of Technical and Scientific Research (CONICET, Argentina). He has worked from 1989 to 1991 at the High Voltage Institute of RWTH, Aachen, Germany. He is at the Instituto de Energía Eléctrica of the University of San Juan, Argentina, as a Lecturer and Researcher since 1982. His main fields of interest are design, modeling and diagnostics of power transformers, asset management, transformer life management, electromagnetic transients in electric machines and networks, modeling of electrical equipment, low frequency electromagnetic fields.